

# DYNAMIC ADSORPTION-DIFFUSION MODEL FOR SIMULATING GAS PRODUCTION IN SHALE

Zehao Yang<sup>1,2</sup>, Qian Sang<sup>1</sup>, Yajun Li<sup>1</sup>, Steven Bryant<sup>2</sup>, Mingzhe Dong<sup>2\*</sup>

1. College of Petroleum Engineering, China University of Petroleum, Qingdao, China 266555; 2. Department of Chemical and Petroleum Engineering, University of Calgary, Calgary, Canada T2N 1N4

*This paper was prepared for presentation at the International Symposium of the Society of Core Analysts held in Trondheim, Norway, 27-30 August 2018*

## ABSTRACT

Reliable mathematical model for analysis of shale gas production requires consideration of gas storage forms in shale rocks: free gas in micro- and nano-scale pores, adsorbed gas on surfaces of organic matter and clay minerals, and dissolved gas in kerogen. In this paper, a dynamic (delayed) adsorption-diffusion (DAD) cylindrical model is presented to analyze gas production process in shale rocks. This model considers that the adsorption/desorption process of adsorbed gas is a time-dependent instead of instantaneously reaching equilibrium. Meanwhile the diffusion process of dissolved gas in kerogen is also taken into account. The exact solution for DAD cylindrical model is derived. The dynamic adsorption/desorption parameters are estimated through fitting the exact solution of DAD cylindrical model with the experimental results of shale gas production process under constant production pressure condition. The parameter estimation method is realized by a global optimization method, called multilevel single-linkage (MLSL) method. The critical points, which distinguish the three domination stages of free gas, adsorbed gas, and dissolved gas, are determined by using DAD model and dissolved gas model. The production characteristics of these three stages are analyzed. The percentage of free gas, adsorbed gas and dissolved gas are also obtained from the DAD cylindrical model analysis.

## INTRODUCTION

The fundamental concept of DAD model has been introduced by Yang et al. in 2016 [1]. The model has been successfully used to analyze experimental results of gas adsorption and desorption in crushed shale samples [2-5]. The DAD model considers the dynamic adsorption/desorption process of methane on the pore surface in kerogen. Meanwhile, it also takes into account the effect of dissolved gas on the production process. Figure 1 is a

SEM image of a shale slice, showing that both nano-pores and micro-pores exist in shale (Figure 1(a)) and that organic matters distribute around inorganic matter in shale (Figure 1(b)).

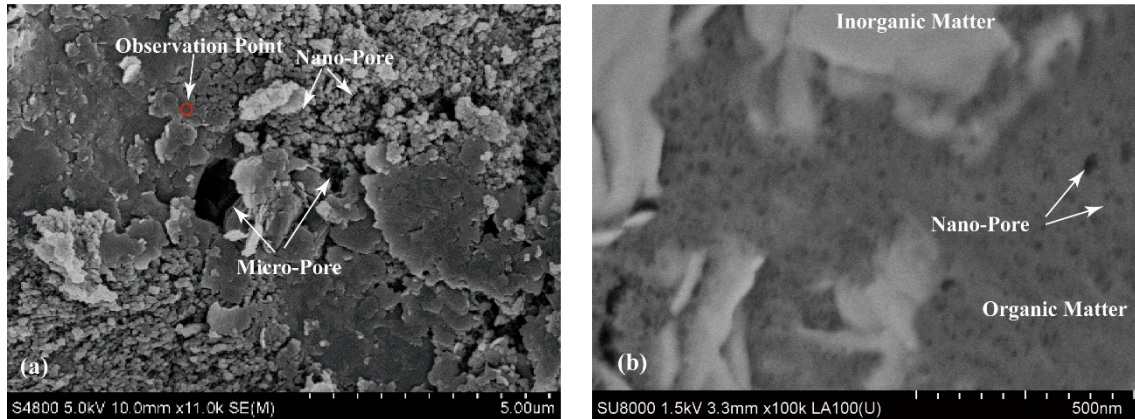


Figure 1: An SEM image [1] displaying (a) distribution of inorganic micro- and nano-pores in inorganic matter and (b) a magnified SEM image of the observation point in (a).

In this paper, the DAD model is expanded to gas production in cylindrical core samples. The schematic of the experimental set-up is shown in Figure 2(a). The radial flow of methane in the core is depicted in Figure 2(b). The gas production process starts when the annulus pressure is suddenly decreased from initial pressure  $P_i$  to production pressure  $P_0$  and maintained constant by BPR. The diameter of shale core is 2.50 cm and its height ( $L$ ) is 5.00 cm. The exact solution of DAD model for radial flow in cylindrical core is developed and used to analyze the experimental results.

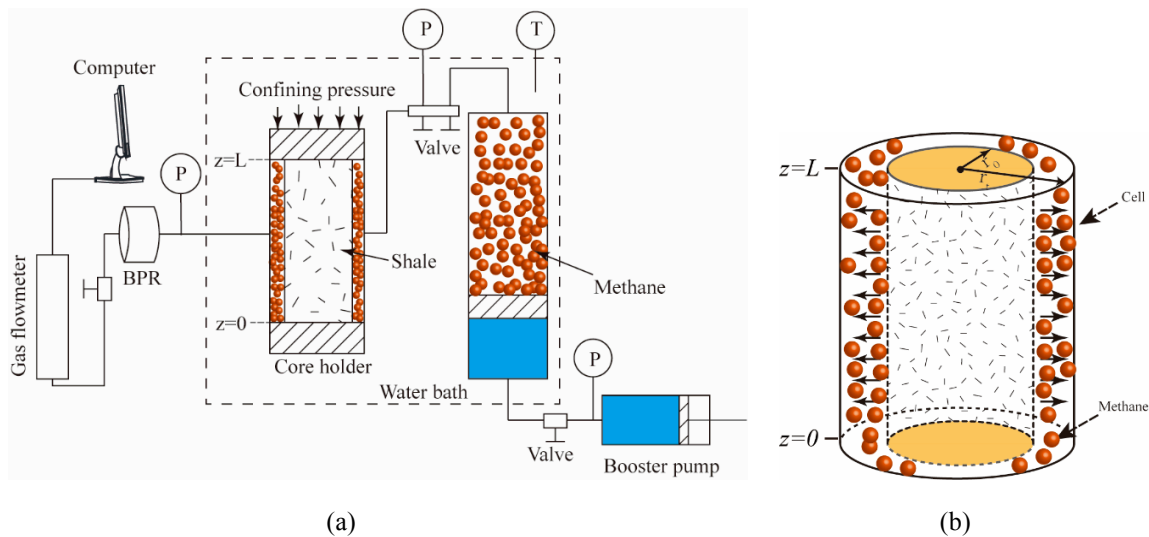


Figure 2: (a) Schematic of experimental setup. (b) Radial flow in the core sample.

## RESULTS

The control equation of the cylindrical DAD model is:

$$\frac{\partial c_f}{\partial t} = \frac{1}{r} \frac{\partial}{\partial r} (D_a r \frac{\partial c_f}{\partial r}) - \frac{\partial c_a}{\partial t} = D_a \left( \frac{\partial^2 c_f}{\partial r^2} + \frac{1}{r} \frac{\partial c_f}{\partial r} \right) - \frac{\partial c_a}{\partial t} \quad (1)$$

The adsorption/desorption rate is expressed as:

$$\frac{\partial c_a}{\partial t} = \kappa = \lambda c_f - \mu c_a \quad (2)$$

In the above two equations,  $c_f$  is concentration of free gas, mol/m<sup>3</sup>;  $c_a$  is the equivalent concentration of adsorbed gas, mol/m<sup>3</sup>;  $D_a$  is apparent diffusion coefficient, m<sup>2</sup>/s;  $\lambda$  is adsorption parameter and  $\mu$  is desorption parameter, s<sup>-1</sup>;  $\kappa$  is adsorption/desorption rate, mol/(m<sup>3</sup>·s);  $r$  is the distance between analyzed point and the axis of the shale core, m; The definitions of  $D_a$ ,  $\lambda$ ,  $\mu$  and  $\kappa$  have been given in literature [1]. The boundary conditions and initial conditions are:

$$c_f \Big|_{r=r_0, t \geq 0} = c_{f0} \quad (3)$$

$$\frac{\partial c_f}{\partial r} \Big|_{r=0, t \geq 0} = 0 \quad (4)$$

$$c_f \Big|_{0 \leq r < r_0, t=0} = c_{fi} \quad (5)$$

$$c_a \Big|_{0 \leq r < r_0, t=0} = c_{ai} \quad (6)$$

where  $c_{f0}$  is constant boundary gas concentration, mol/m<sup>3</sup>;  $c_{fi}$  is initial free gas concentration, mol/m<sup>3</sup>;  $c_{ai}$  is initial adsorbed gas concentration, mol/m<sup>3</sup>.

The exact solution of the model is:

$$c_f = c_{f0} + \sum_{n=1}^{\infty} \frac{(c_{f0} - c_{fi}) I_0(k(a_n)r) e^{a_n t}}{a_n r_0 I(1, k(a_n)r_0) \frac{a_n^2 + 2a_n \mu + \mu(\lambda + \mu)}{2k(a_n)D_a(a_n + \mu)^2}} \quad (7)$$

$$c_a = c_{a0} + \sum_{n=1}^{\infty} \frac{(c_{a0} - c_{ai}) I_0(k(a_n)r) \mu e^{a_n t}}{a_n r_0 I(1, k(a_n)r_0) \frac{a_n^2 + 2a_n \mu + \mu(\lambda + \mu)}{2k(a_n)D_a(a_n + \mu)^2} (a_n + \mu)} \quad (8)$$

where  $a_n$  is the  $n$ th root of:

$$I_0(k(a_n)r_0) = 0 \quad (9)$$

$k(a_n)$  is equal to  $\sqrt{\frac{a_n(\lambda + \mu + a_n)}{D_a(a_n + \mu)}}$ , and  $I_0(x)$  is modified Bessell function with an order of zero.

Integrating the total concentration from the surface of the core to its center along the radial direction gives the amount of produced gas at an arbitrary time as:

$$M_t = \int_0^{r_0} (c_{fi} + c_{ai} - c_f - c_a) \cdot 2\pi r L \phi dr$$

$$= \frac{r_0^2 (c_i - c_0) \pi (\lambda + \mu) L \phi}{\mu} + \sum_{n=1}^{\infty} \frac{4(c_{ai} - c_{a0}) D_a e^{a_n t} \pi (a_n + \mu) (a_n + \mu + \lambda) \phi}{a_n (a_n^2 + 2a_n \mu + \mu(\lambda + \mu))} \quad (10)$$

When the time approaches infinity (i.e., at an equilibrated steady state), the total accumulative produced gas is:

$$M_{\infty} = \frac{r_0^2 (c_i - c_0) \pi (\lambda + \mu) L \phi}{\mu} \quad (11)$$

The residual mass fraction ( $F_R$ ) is defined as the ratio of the residual gas that will be produced from the shale core to the accumulative gas that eventually will be produced from the sample:

$$F_R = 1 - \frac{M_t}{M_{\infty}} = \sum_{n=1}^{\infty} \frac{-4D_a e^{a_n t} \mu (a_n + \mu) (a_n + \mu + \lambda)}{a_n r_0^2 (\lambda + \mu) (a_n^2 + 2a_n \mu + \mu(\lambda + \mu))} \quad (12)$$

The accuracy of the exact solution Eq. (12) has been verified through numerical solution. The numerical method used is finite difference method. The comparison is shown in

Figure 3(a).

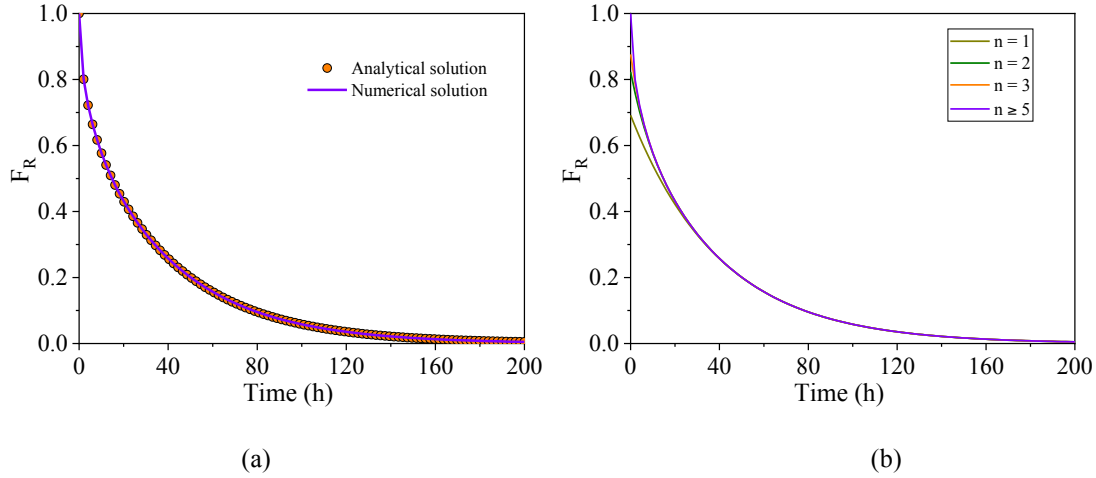


Figure 3: (a) Comparison of analytical solution and numerical solution calculated from FDM for DAD model. (b) Convergence of the approximate solution of DAD cylindrical model.

The analytical solution is in the form of an infinite series and therefore may be difficult to use in practice. The common strategy to deal with such an issue is to test the number of terms needed to approximate the exact solution. It can be seen from Figure 3(b) that when  $n$  is equal to or greater than 5,  $F_R$  is almost the same with the exact solution. Therefore, the approximate solution is given as:

$$F_R \approx \sum_{n=1}^5 \frac{-4D_a e^{a_n t} \mu (a_n + \mu)(a_n + \mu + \lambda)}{a_n r_0^2 (\lambda + \mu)(a_n^2 + 2a_n \mu + \mu(\lambda + \mu))} \quad (13)$$

The approximate solution can be used to analyze gas production data obtained from laboratory gas production experiments. Figure 4 shows a cumulative shale gas production curve in a shale core sample. From Figure 4, it can be seen that several stages may exist in the shale gas production process. At about 5 hours, the cumulative production curve begins to increase again. Most of our experimental results have this phenomenon. It is because there may be a threshold pressure in the inorganic pore [1, 5]. When the gas pressure is smaller than this value, the gas in the organic matter (kerogen) almost won't come out due to the nanopores of kerogen are closed. It can also be found that the production of dissolved gas in kerogen is much slower than that of free gas and adsorbed gas. Therefore, the experimental data in Figure 4 is divided into and analyzed as two parts.

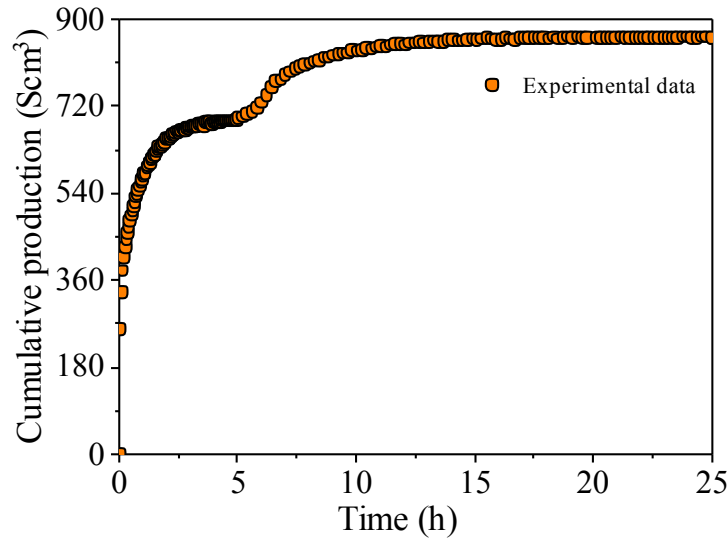


Figure 4: Cumulative gas production result in a cylindrical shale core sample.

DAD cylindrical model (Eq. (13)) is first used to fit the data in the first 5 hours and the result is shown in Figure 5(a). The regression method is MLSL global optimization method, which has been introduced in detail in [1]. Diffusion coefficient ( $D_a$ ), adsorption parameter ( $\lambda$ ), desorption parameter ( $\mu$ ) are obtained as  $1.03 \times 10^{-7} \text{ m}^2/\text{s}$ ,  $2.31 \times 10^{-4} \text{ s}^{-1}$  and  $3.04 \times 10^{-4} \text{ s}^{-1}$ , respectively.

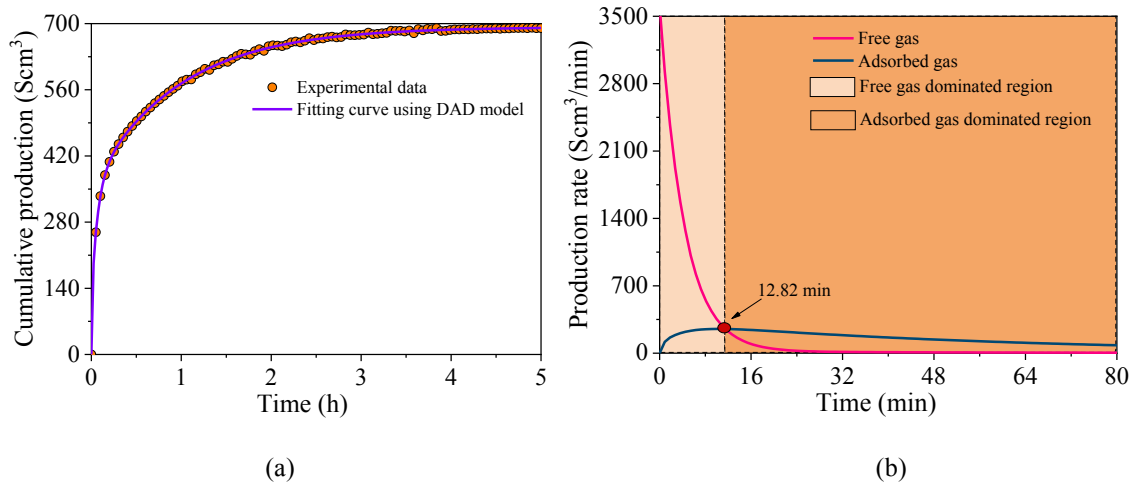


Figure 5: (a) Fitting result of cumulative production vs time in first 5 hours. (b) The production rates of free gas and adsorbed gas based on fitting results of the experiment.

Using the estimated results above, the production rate of free gas and adsorbed gas in the first 5 hours can be further obtained through DAD cylindrical model (Eq. (7)-Eq. (8)). The analyzed result is shown in Figure 5(b). It is found that the first 5 hour production

can be further divided into two stages. In the first stage, free gas expansion is the main production mechanism. This stage is fast and short. After 12.8 minutes, the production of the adsorbed gas dominates the process and lasts much longer than the first stage.

After 5 hours, the release of the dissolved gas dominates the production process. The production of dissolved gas is much slower than the two former stages (see Figure 4). It is proper to assume that the pore pressure is constant and equal to the boundary pressure in this stage [6]. This process is depicted schematically in Figure 6(a). The accumulative gas production in this stage can be obtained through a plane diffusion model [5]:

$$M_{dt} = M_{d\infty} \left( 1 - \sum_{n=0}^{\infty} \frac{8}{(2n+1)^2 \pi^2} e^{-\frac{D_d(2n+1)^2 \pi^2 t}{4h^2}} \right) \quad (14)$$

where  $M_{d\infty}$  is the total accumulative dissolved gas,  $\text{Scm}^3$ , which can be obtained through experimental result (Figure 4);  $D_d$  is the diffusion coefficient of dissolve gas in kerogen,  $\text{m}^2/\text{s}$ ;  $h$  is the thickness of organic matter around the pores,  $\text{nm}$ , which can also be obtained through experimental data [6]. For the experimental data presented in Figure 4, the thickness  $h$  is 121  $\text{nm}$ .

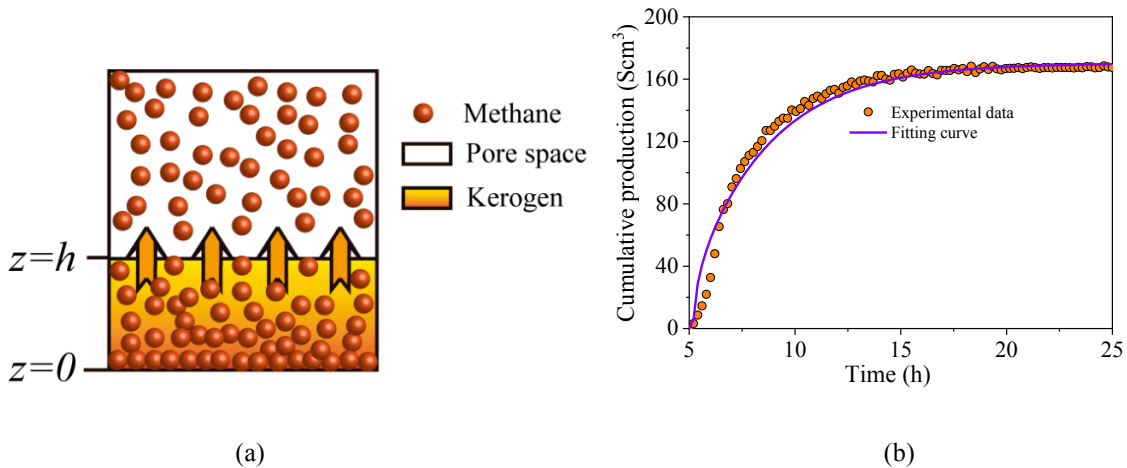


Figure 6: (a) Schematic of the diffusion process of the dissolved gas in organic matter. (b) Fitting result of cumulative production vs time after 5 hours.

Using the plane diffusion model (Eq. (14)) to fit with the experimental data after 5 hours (Figure 4), the result is obtained as shown in Figure 6(b). The diffusion coefficient ( $D_d$ ) of the dissolved gas in kerogen is about  $5.26 \times 10^{-19} \text{m}^2/\text{s}$ , which is much smaller than the apparent diffusion coefficient ( $D_a$ ).

From the above analysis results, it can be found that there are two critical points and three stages in the gas production process as shown in Figure 7. Before first critical point, free gas is the dominant gas; in the second region adsorbed gas is the dominant gas; after the second critical point, dissolved gas becomes the dominant gas.

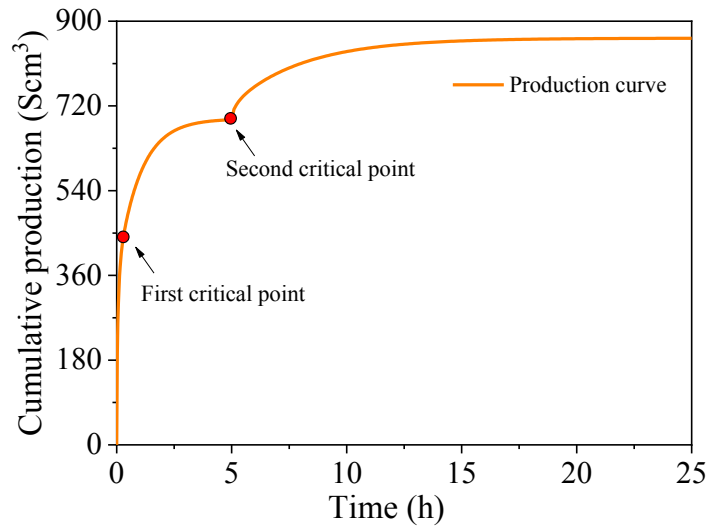


Figure 7: Simulated gas production curve using DAD cylindrical model.

Based on the analysis using DAD cylindrical model, the percentage of each form of stored gas in shale is obtained and shown in Figure 8. It can be seen that in the shale core tested (Figure 4) the percentage of stored free gas, adsorbed gas, and dissolved gas is 45.2%, 34.8% and 20%, respectively.

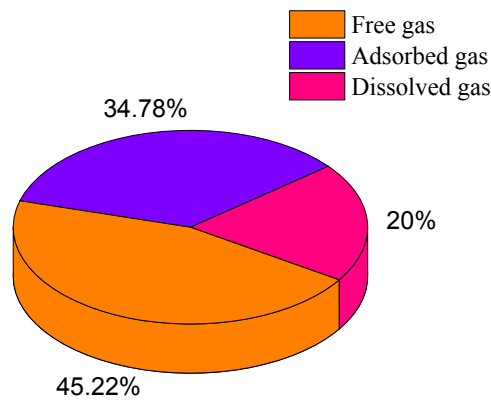


Figure 8: The percentage of free gas, adsorbed gas and dissolved gas during production process.



## CONCLUSIONS

In this paper, we presented the exact solution of DAD cylindrical model and used it to analyze the corresponding experimental data. It is found that the production of shale gas can be divided into three stages. In the first stage, free gas is the dominant gas. The production process is fast and short. In the second stage, adsorption gas is the dominant gas. The production rate is smaller and the production time is longer than in the first stage. The third stage is dominated by the dissolved gas. The production rate in this stage is much smaller and the production time is much longer than in the former two stages. Meanwhile, the percentage of three forms of stored gas — free gas, adsorbed gas and dissolved gas — can also be obtained from the DAD model analysis.

## ACKNOWLEDGEMENTS

This work was supported by National Key Basic Research Program of China (973 Program) (No. 2014CB239103), Natural Science Foundation of China (51774310), Canada Excellence Research Chair (CERC), Mitacs (Canada) and China University of Petroleum (East China) Postgraduate Innovation Project (No. YCX2017018)

## REFERENCES

- [1] Yang Z.H., Wang W.H., Dong M.Z., et al. A model of dynamic adsorption–diffusion for modeling gas transport and storage in shale. *Fuel*, (2016) 173: 115-128.
- [2] Wang J.J., Li Y.J., Yang Z.H., et al. Measurement of dynamic adsorption–diffusion process of methane in shale. *Fuel*, (2016) 172: 37-48.
- [3] Wang J.J., Yang Z.H., Dong M.Z., et al. Experimental and numerical investigation of dynamic gas adsorption/desorption–diffusion process in shale. *Energy & Fuels*, (2016) 30(12): 10080-10091.
- [4] Wang J.J., Dong M.Z., Yang Z.H., et al. Investigation of methane desorption and its effect on the gas production process from shale: experimental and mathematical study. *Energy & Fuels*, (2016) 31(1): 205-216.
- [5] Sang Q., Li Y.J., Yang Z.H., et al. Experimental investigation of gas production processes in shale. *International Journal of Coal Geology*, (2016) 159: 30-47.
- [6] Etminan S.R., Javadpour F., Maini B.B., et al. Measurement of gas storage processes in shale and of the molecular diffusion coefficient in kerogen. *International Journal of Coal Geology*, (2014) 123: 10-19.